Trajectory Tracking Control of USV Based on Exponential Global Fast Terminal Sliding Mode Control

Tengbin Zhu (pigtb1990@163.com)
Shanghai Maritime University https://orcid.org/0000-0003-4003-120X
Yingjie Xiao
Shanghai Maritime University
Hao Zhang
Shanghai Maritime University
Yufeng Pan
Shanghai Maritime University

Research Article

Keywords: trajectory tracking, unmanned surface vessel, backstepping, exponential sliding mode, Lyapunov

Posted Date: January 19th, 2022

DOI: https://doi.org/10.21203/rs.3.rs-1234209/v1

Noname manuscript No.
(will be inserted by the editor)

Trajectory tracking control of USV based on exponential global fast terminal sliding mode control

Tengbin Zhu · Yingjie Xiao · Hao Zhang · Yufeng Pan

Received: date / Accepted: date

Abstract This paper studies the trajectory tracking of an under-driven surface unmanned surface vessel (USV). The trajectory tracking controller is divided into two parts: the kinematics controller and the dynamic controller. Taking the hull coordinate system of the USV as the datum plane, the kinematics controller is designed based on the backstepping method, and the virtual control input of the speed and the heading deviation of the ship is obtained. A dynamic controller is designed through an exponential sliding surface to stabilize the error of speed and heading deviation, thereby stabilizing the position error. In the process of designing the controller, the stability of the entire closed-loop control system is analyzed though using Lyapunov's stability theory. Finally, the designed numerical simulation experiment is carried out. The proposed exponential sliding mode controller is compared with the ordinary sliding mode controller, and it is verified that the proposed controller has better effectiveness and robustness in the trajectory tracking of the under-actuated USV. Insert your abstract here. Include keywords, PACS and mathematical subject classification numbers as needed.

Keywords trajectory tracking · unmanned surface vessel · backstepping · exponential sliding mode · Lyapunov

Tengbin Zhu
Merchant Marine College, Shanghai Maritime University, Shanghai 201306, China
E-mail: pigtb1990@163.com

Yingjie Xiao
Merchant Marine College, Shanghai Maritime University, Shanghai 201306, China

1 Introduction

Unmanned surface vessel (USV) can perform tasks in various unknown and complex surface environments due to its autonomy, intelligence, and modularity. It is widely used in meteorological watermark measurement, island coke surveying and mapping, marine pollution prevention, rescue, subsea exploration and other dangerous missions with high coefficients and harsh environments[1, 2,3,4]. Research on trajectory tracking and control of under-driven USV has received wide attention in recent years. Trajectory tracking control means that the ship reaches the target position within a specified time according to the route designed by the planner, so as to realize the safe and efficient operation of the ship. Generally speaking, USV have no lateral propulsion, which makes its motion model under-driving. At the same time, the external interference and the unmodeled part of the dynamic system make the USV have unpredictable non-linear characteristics, which makes it extremely difficult to carry out trajectory tracking control. At present, the main methods of under-actuated USV trajectory tracking control include feedback linearization method, predictive control method, backstepping method and sliding mode control.

The feedback linearization method can simplify the complex model and easy to adjust the parameters. literature [5] proposed a simple state feedback control law, and proved that the control law can make the tracking error dynamic and global exponentially stable, and carried out the ship model experiment. literatures [6] and [7] determined a forehand position on the USV, controlled the movement of this point along the trajectory based on the input-output feedback linearization method. However, the feedback linearization method requires a more accurate mathematical model. If the

mathematical model cannot be accurately established, the part that has a greater impact on the system will cause the controller to fail to stabilize the system.

The predictive control algorithm is convenient to support various constraint conditions, and predictive fitting is performed as much as possible through rolling optimization, which has a good control effect. literature [8] proposed a robust adaptive autopilot based on model predictive controller (MPC), which can handle sudden changes in system dynamics. literature [9] used differential homomorphism and state-dependent Riccati equation (SDRE) theory to design the control law for the under-driven surface ship with limited input, and used the convex optimization method to solve the constrained control input of the system. In literature [10], a nonlinear model predictive control is proposed, system constraints on inputs, input increments, and outputs are incorporated into the NMPC framework. literature [11] proposed an MPC scheme with line-of-sight path generation capability, using a quadratic programming method to solve the ship's LOS model linearization. But the predictive control algorithm requires a lot of computing power because it needs a lot of online optimization.

Backstepping is a control method based on the idea of compensation, which decomposes a complex system into simpler subsystems, and then reversely controls the system by introducing virtual control variables. It is often used to combine with other controls. In literature [12], the design and simulation implementation of a nonlinear controller for underactuated USV based on the command filter backstepping method is introduced. literature [13] proposed a backstepping control algorithm based on state feedback, adding an overall action to the controller to further enrich the steady-state performance and control accuracy of the USV trajectory tracking control system.

In recent years, the sliding mode control method has received extensive attention from scholars due to its insensitivity and robustness to parameter changes, and studies on its application in the industrial field [14,15]. Structure change of sliding mode control has nothing to do with the object parameters and disturbances. Instead, the current state is used to adjust the structure to force the system state to enter the sliding mode surface and gradually stabilize along the sliding mode surface. literature [16] introduced some sliding variables with relative degrees to three different types of under-actuated systems. literature [17] proposed a robust sliding mode control method with disturbance observer and state observer, which achieved robust control of disturbances by controlling the angle of the water jet system. literature [18] combines backstepping control and sliding mode control to improve the robustness of the unmanned submarine under system uncertainty and environmental interference. However, due to the *sgn* function discontinuous switching of traditional sliding mode control, chattering exists in the initial state. In terms of eliminating chattering, In the [19] introducing a continuous differentiable approximate saturation function, and literature [20] constructs a continuous adaptive term to reduce the system chattering phenomenon.

The traditional sliding mode memory has good robustness, but there is a problem of convergence in unknown time. In order to suppress chattering and overcome the unknown time convergence problem of traditional sliding mode control, literature [21] proposed terminal sliding mode control. But when the system is far from the equilibrium point, the convergence speed of ordinary terminal sliding mode control is lower than that of traditional sliding mode. Some scholars have proposed global terminal sliding mode control, which enables the system to converge quickly under the combined action of linear and nonlinear surfaces. literature [22] applies global terminal sliding mode control to the stabilization of USV.

However, the new global terminal sliding mode control currently mainly used in single-input single-output systems, not get applied in under-driving systems, especially high-order under-driving systems. In this paper, combined with the exponential terminal sliding mode control surface [23,24], a new under-actuated USV trajectory tracking control method is proposed. Firstly mathematical model in inertial coordinate system is converted into hull coordinate system to facilitate calculation. Secondly through the analysis of the Lyapunov stability criterion based on the horizontal and vertical coordinate positions, the virtual control quantity of ard speed and the virtual control quantity of heading error are determined. Then analysis and deduction based on the exponential terminal dynamic sliding mode, determine the exponential terminal sliding mode control law that satisfies the second-order dynamic system. Lastly verify the algrithm effectiveness through numerical experiments compared with compared with the global integral sliding mode controller.

The main contributions of the job in this paper can be summarized as follows:

(1) Using the hull coordinate system as the reference plane, the virtual control value of the under-actuated USV is determined by the backstepping method and the Lyapunov criterion.
(2) Exponential terminal sliding mode is applied to multi-output multi-output underactuated system and a second-order exponential terminal sliding mode con-

troller is constructed to improve the trajectory tracking capability of USV.

(3) Compared with the global integral sliding mode controller in the numerical test, results show that the proposed control method can not only converge rapidly, but also restrain chattering effectively due to no switching surface.

The organization structure of this paper is as follows: Section 2 introduces the motion mathematical model of USV. Section 3 designs the virtual control variables through the reverse step method base on the hull coordinate system as the reference coordinate. Section 4 uses the exponential sliding surface to design control laws. In Section 5, comparative simulation experiments are conducted to prove the superiority of the controller in this paper. Section 6 makes a simple summary.

2 Mathematical model of USV

2.1 Kinematics Model

The USV has 6 degrees of freedom. When considering the trajectory tracking control of the USV, this paper refers to reference [25], only three degrees of freedom, namely pitch, yaw and bow roll need to be considered. It is assumed that the USV is symmetric, the diagram of the 3 degree of freedom (3-DOF) plane coordinate system is shown in Fig. 1.

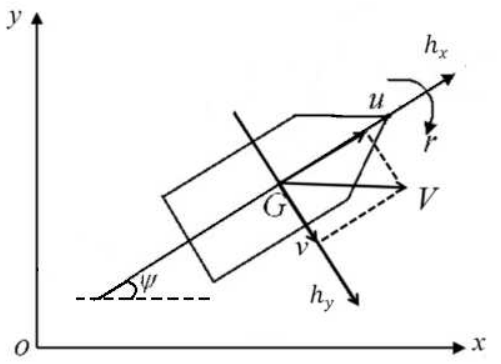

Fig. 1 Schematic diagram of 3-DOF coordinate of USV

Among them, $o-xy$ represents the fixed coordinate system of the earth, $G-h_xh_y$ represents the hull coordinate system of the USV, its moving speed is V, which can decompose in the attached coordinate system, and the component on the h_y axis is v , which is the lateral speed of the USV, and the component in the h_x axis direction is u, which is the longitudinal speed of the USV. ψ represents the heading angle, and θ represents the angular velocity.

Through analysis, the simplified kinematics model of USV can be obtained as follows:

$$\dot{\eta} = J(\psi)v \tag{1}$$

Among them, $\eta = [x, y, \psi]^T, v = [u, v, r]^T$. $J(\psi)$ represents the rotation matrix from the hull coordinate system to the inertial coordinate system, the expression is as follows:

$$J(\psi) = \begin{bmatrix} \cos\psi & -\sin\psi & 0 \\ \sin\psi & \cos\psi & 0 \\ 0 & 0 & 1 \end{bmatrix} \tag{2}$$

Where $J(\psi)^{-1} = J(\psi)^T$ can be derived, and the state space expression of the kinematics model of the USV is expressed as:

$$\begin{cases} \dot{x} = u\cos\psi - v\sin\psi \\ \dot{y} = u\sin\psi + v\cos\psi \\ \dot{\varphi} = r \end{cases} \tag{3}$$

2.2 Dynamics model

The dynamics mathematical model of the USV can be described as:

$$M\dot{v} + C(v)v + Dv + \tau_d = \tau \tag{4}$$

Where $M = diag\{m_{11}, m_{22}, m_{33}\}$ is the additional inertia matrix, $D = diag\{d_{11}, d_{22}, d_{33}\}$ is the hydrodynamic damping parameter matrix. η and v are consistent as above. $\tau = [\tau_1, 0, \tau_3]^T$, τ_1 and τ_3 are the longitudinal propulsion and steering moment, respectively. $C(v)$ is the Coriolis and centripetal force matrix, $\tau_d = [\tau_{1dis}, \tau_{2dis}, \tau_{3dis}]^T$, τ_1 is the disturbances of the unmodeled parts and environment such as wind, waves, currents, etc. τ_{1dis}, τ_{2dis} and τ_{1dis} are the disturbance forces and moments in the longitudinal, lateral, and steering angles, respectively. Then the state-space equation expression of the USV's horizontal dynamics model:

$$\begin{cases} \dot{u} = \frac{m_{22}}{m_{11}}vr - \frac{d_{11}}{m_{11}}u + \frac{\tau_u + \tau_{1dis}}{m_{11}} \\ \dot{v} = -\frac{m_{11}}{m_{22}}ur - \frac{d_{22}}{m_{22}}v + \frac{\tau_{2dis}}{m_{22}} \\ \dot{r} = \frac{m_{11}-m_{22}}{m_{33}}uv - \frac{d_{33}}{m_{33}}r + \frac{\tau_r + \tau_{3dis}}{m_{33}} \end{cases} \tag{5}$$

Among them, the disturbance is satisfied with $|\tau_{1dis}| \leq \tau_{1\max} < +\infty$, $|\tau_{2dis}| \leq \tau_{2\max} < +\infty$, $|\tau_{3dis}| \leq \tau_{3\max} < +\infty$.

2.3 Motion model in hull coordinate system

According to Eq. (2) the kinematics model of USV, the formula for transforming the inertial coordinate system into the hull coordinate system can be obtained as follows:

$$\begin{bmatrix} h_x \\ h_y \\ h_r \end{bmatrix} = \begin{bmatrix} \cos\psi & \sin\psi & 0 \\ -\sin\psi & \cos\psi & 0 \\ 0 & 0 & 1 \end{bmatrix} \begin{bmatrix} x \\ y \\ r \end{bmatrix} \tag{6}$$

Let USV's longitudinal coordinate, transverse coordinate, heading angle, longitudinal speed, transverse speed and angular speed in the hull coordinate system as:

$$\begin{aligned} &(h_1, h_2, h_3, h_4, h_5, h_6) \\ &= (x\cos\psi + y\sin\psi, -x\sin\psi + y\cos\psi, \psi, u, v, r) \end{aligned} \tag{7}$$

The differential homeomorphism transformation is performed on the unmanned vessel system, and the new state space equation is obtained as:

$$\begin{cases} \dot{h}_1 = h_4 + h_2 h_6 \\ \dot{h}_2 = h_5 - h_1 h_6 \\ \dot{h}_3 = h_6 \\ \dot{h}_4 = w_1 \\ \dot{h}_5 = w_2 \\ \dot{h}_6 = w_3 \end{cases} \tag{8}$$

Among them, w_1, w_2 and w_3 are the conversion of control input and disturbance synthesis, the formula is as follows:

$$\begin{cases} w_1 = \frac{m_{22}}{m_{11}} h_5 h_6 - \frac{d_{11}}{m_{11}} h_4 + \frac{(\tau_u + t_{1dis})}{m_{11}} \\ w_2 = \frac{m_{11}}{m_{22}} h_4 h_6 - \frac{d_{11}}{m_{22}} h_5 + \frac{t_{2dis}}{m_{22}} \\ w_3 = \frac{(m_{11} - m_{22})}{m_{33}} h_4 h_6 - \frac{d_{33}}{m_{33}} h_6 + \frac{(\tau_r + t_{3dis})}{m_{33}} \end{cases} \tag{9}$$

Because w_1 and w_3 can be controlled by τ_u and τ_r directly, respectively. w_2 is related to w_1 and w_3, let $w_1 = t_u$, $w_3 = t_r$, we can get the final state space equation of USV in the hull coordinate system as:

$$\begin{cases} \dot{h}_1 = h_4 + h_2 h_6 \\ \dot{h}_2 = h_5 - h_1 h_6 \\ \dot{h}_3 = h_6 \\ \dot{h}_4 = t_u \\ \dot{h}_5 = -B * h_5 - A * h_4 * h_6 + T_{2dis} \\ \dot{h}_6 = t_r \end{cases} \tag{10}$$

3 Virtual control design based on Lyapunov

3.1 Lyapunov in the hull coordinate system

According to the second method of Lyapunov, the asymptotic stability of the system can be proved. In order to make the system eventually uniformly asymptotically stable, define the Lyapunov function in the inertial coordinate system:

$$V_o = \frac{1}{2}\left(x_e^2 + y_e^2\right) \tag{11}$$

Among them, the coordinate error of the USV is $\begin{bmatrix} x_e \\ y_e \end{bmatrix} = \begin{bmatrix} x - x_r \\ y - y_r \end{bmatrix}$, x_r and y_r are the coordinates of the reference trajectory in the x and y axis of the inertial coordinate system respectively. Eq. (11) can be equivalent to equation as below:

$$V = \frac{1}{2}\left(h_{xe}^2 + h_{ye}^2\right) \tag{12}$$

Where h_{xe} and h_{ye} represent the longitudinal and lateral coordinate errors of the USV in the hull coordinate system respectively, and they can be proved as below.

Proof. In order to facilitate calculations, we can set $A = \begin{bmatrix} \cos\psi & \sin\psi \\ -\sin\psi & \cos\psi \end{bmatrix}$, then A is an invertible matrix, $A^{-1} = A^T$. The transformation of x_r and y_r in the hull coordinate system is

$$\begin{bmatrix} x_r \\ y_r \end{bmatrix} = \mathrm{A}^{\mathrm{T}} \begin{bmatrix} h_{1r} \\ h_{2r} \end{bmatrix} \tag{13}$$

Then, the coordinate error in the inertial coordinate system can be expressed as:

$$\begin{bmatrix} x_e \\ y_e \end{bmatrix} = \mathrm{A}^{\mathrm{T}} \begin{bmatrix} h_1 - h_{1r} \\ h_2 - h_{2r} \end{bmatrix} = \mathrm{A}^{\mathrm{T}} \begin{bmatrix} h_{xe} \\ h_{ye} \end{bmatrix} \tag{14}$$

Therefore, the original Lyapunov function can be transformed into the Lyapunov function in hull coordinates as

$$V_o = \frac{1}{2}\left[h_{xe} h_{ye}\right] \mathrm{A}\mathrm{A}^{\mathrm{T}} \begin{bmatrix} h_{xe} \\ h_{ye} \end{bmatrix} = \frac{1}{2}\left(h_{xe}^2 + h_{ye}^2\right) \tag{15}$$

3.2 Virtual control quantity design

According to the kinematics model in section 2.1, let the heading of the reference trajectory be $\psi_r = \arctan\frac{\dot{y}_r}{\dot{x}_r}$, and the kinematics model of the reference trajectory is

$$\begin{cases} \dot{x}_r = u_r\cos\psi_r - v_r\sin\psi_r \\ \dot{y}_r = u_r\sin\psi_r + v_r\cos\psi_r \\ \dot{\psi}_r = r_r \end{cases} \tag{16}$$

According to Eqs. (7) and (8) to transform the coordinates of the reference point to

$$\begin{cases} h_{1r} = x_r\cos(\psi) + y_r\sin(\psi) \\ h_{2r} = -x_r\sin(\psi) + y_r\cos(\psi) \end{cases} \tag{17}$$

Carrying out the first-order differentiation on the time of Eq. (17), we get

$$\begin{cases} \dot{h}_{1r} = \dot{x}_r\cos(\psi) - x_r r\sin(\psi) + \dot{y}_r\sin(\psi) + y_r r\cos(\psi) \\ \dot{h}_{2r} = -\dot{x}_r\sin(\psi) - x_r\cos(\psi) + \dot{y}_r\cos(\psi) - y_r r\sin(\psi) \end{cases} \tag{18}$$

Organizing the Eq. (18) to get

$$\begin{cases} \dot{h}_{1r} = h_{4r} + h_{2r}h_6 \\ \dot{h}_{2r} = h_{5r} - h_{1r}h_6 \\ h_{4r} = \dot{x}_r\cos(\psi) + \dot{y}_r\sin(\psi) \\ h_{5r} = -\dot{x}_r\sin(\psi) + \dot{y}_r\cos(\psi) \end{cases} \tag{19}$$

From $h_{xe} = h_1 - h_{1r}$,$h_{ye} = h_2 - h_{2r}$, then $\dot{h}_{xe} = \dot{h}_1 - \dot{h}_{1r}$, $\dot{h}_{ye} = \dot{h}_2 - \dot{h}_{2r}$, combine Eqs. (7), (8), (19) to get Eq. (20) as below:

$$\begin{cases} \dot{h}_{xe} = H_4 + h_{ye}h_6 \\ \dot{h}_{ye} = H_5 - h_{xe}h_6 \\ H_4 = h_4 - h_{4r} \\ H_5 = h_5 - h_{5r} \end{cases} \tag{20}$$

After Taking the time derivative of equation (12), then combining Eq. (20) to obtain

$$\dot{V} = h_{xe}H_4 + h_{ye}H_5 \tag{21}$$

After substituting Eqs. (7) and (19) into Eq. (21), expand into

$$\begin{aligned} \dot{V} =& h_{xe}\left(u - \left(\dot{x}_r\cos\psi + \dot{y}_r\sin\psi\right)\right) \\ &+ h_{ye}\left(v - \left(-\dot{x}_r\sin\psi + \dot{y}_r\cos\psi\right)\right. \end{aligned} \tag{22}$$

Let $\psi_e = \psi - \psi_r$, then $\psi = \psi_e + \psi_r$, according to the trigonometric function combination Eq. (16), we can get

$$\begin{aligned} \dot{V} =& h_{xe}\left(u - u_r\cos\psi_e - v_r\sin\psi_e\right) \\ &+ h_{ye}\left(v - v_r\cos\psi_e + u_r\sin\psi_e\right) \end{aligned} \tag{23}$$

Because $\tan\psi_r = \frac{\sin\psi_r}{\cos\psi_r} = \frac{\dot{y}_r}{\dot{x}_r}$ is substituting into Eq. (16), $v_r = 0$ can be obtained, so

$$\dot{V} = h_{xe}\left(u - u_r\cos\psi_e\right) + h_{ye}v + h_{ye}u_r\sin\psi_e \tag{24}$$

Taking the USV pl speed and heading deviation solution as the virtual control input of the kinematics model sub-controller, and combined $\psi_e = \psi - \psi_r$, its expected value can be designed as follows:

$$\begin{cases} u_d = -k_1 h_{xe} + u_r\cos\psi_e \\ \psi_d = -\arcsin\left(k_2 h_{ye}u_r\right) + \psi_r \end{cases} \tag{25}$$

Among them, k_1 and k_2 are the adjustable gain coefficients, which needs to be satisfied with $k_1 > 0$, $k_2 > 0$. Because the value of the trigonometric sine function is [-1,1], then require $-1 \le k_2 h_{ye}u_1 \le 1$. When the tracking error h_{xe}, h_{ye} and ψ_e are all zero, the virtual control input u_d and ψ_d are respectively equal to the expected thruster speed u_r and the expected ship heading ψ_r. Because $sgn(\sin\psi_e) = sgn(\tan\psi_e)$, so in the case $k_1 > 0$, $k_2 > 0$, only set the virtual control input as:

$$\begin{cases} u_d = -k_1 h_{xe} + u_r\cos\psi_e \\ \psi_d = -\arctan\left(k_2 h_{ye}u_r\right) + \psi_r \end{cases} \tag{26}$$

Then, substituting u_d and ψ_d into Eq. (24), we can get

$$\dot{V} = -k_1 h_{xe}^2 + h_{ye}v - k_2\tan^2\psi_e \tag{27}$$

Considering that u_d and ψ_d are not really controllable variables, the dynamic control law and the auxiliary control law should be designed to ensure that $\dot{V}$ are negative, so that h_{xe} and h_{ye} are finally stabilized.

Let $V_v = \frac{1}{2}v^2$, combine the values $\dot{v}$ in Eqs. (7) and (10) to differentiate in time to obtain

$$\dot{V}_v = v\left(-Bv - Aur + T_{2dis}\right) \tag{28}$$

Because the value of B and A are larger than 0, when $|v| > \left(Aur - T_{2dis}\right)/B$, $|v|$ is decreasing, i.e. $dotV < 0$. So when T_{2dis} is bounded, v can be regarded as absolutely bounded, that is

$$|v| \leq |(Aur - T_{2dis})| / B \tag{29}$$

Since the lateral movement of the USV is mainly produced by the angular velocity r. when ψ_e tends to 0, r also tends to 0, then v also tends to 0, so $h_{ye}v$ can be stabilized by adjusting k_2 in the third term of Eq. (24). And finally make $\dot{V}$ a negative value, so v can be regarded as $v \approx 0$ [26].

4 Exponential sliding mode controller

4.1 Exponential terminal sliding mode

The exponential terminal sliding mode control has a fast asymptotic tracking effect and anti-buffing effect. The first-order dynamic system sliding mode surface [23,24] is

$$S = \dot{x} + \frac{\alpha}{k}\left(e^{k|x|} - 1\right) sgn(x) + \frac{\beta}{k}\left(1 - e^{-k|x|}\right)^{q/p} e^{k|x|} sgn(x) \tag{30}$$

In the Eq. (30), $x \in R$, $\alpha > 0$, $\beta > 0$; p and q are all positive odd numbers, and p is larger than q; $0 < k \leq 1$.

According to Eq. (30), when $S = 0$, the convergence time is

$$t_s = \frac{p}{\alpha(p-q)} \ln \frac{\alpha\left(1 - e^{-k|x(0)|}\right)^{(p-q)/p} + \beta}{\beta} \tag{31}$$

The convergence time of fast terminal sliding mode control [24] is

$$t_{s1} = \frac{p}{\alpha(p-q)} \ln \frac{\alpha|x(0)|^{(p-q)/p} + \beta}{\beta} \tag{32}$$

On the exponential terminal sliding mode, the system is gradual and stable, and at the same time it takes a faster time to reach the equilibrium point than t_{s1}.

4.2 Control law design

In order to make the USV's thruster speed and heading angle reach the desired value, it is necessary to design the auxiliary control laws so that the thruster speed tracking error and the heading angle tracking error eventually approach zero. The thruster speed error and heading angle error are defined as follows:

$$u_E = u - u_d, \psi_E = \psi - \psi_d \tag{33}$$

(A) Propulsion control law τ_u design

In order to stabilize the thruster speed error u_E, the exponential global terminal sliding mode dynamic surface is selected as:

$$\begin{aligned} S_{u1} =& \dot{u}_E + \frac{\alpha_0}{k_{u1}}\left(e^{k_{u1}|u_E|} - 1\right) sgn\left(u_E\right) \\ &+ \frac{\beta_0}{k}\left(1 - e^{-k_{u1}|u_E|}\right)^{q_0/p_0} e^{k_{u1}|u_E|} sgn\left(u_E\right) \end{aligned} \tag{34}$$

Taking the time derivative of u_E, combined with Eq. (5), we can get

$$\dot{u}_E = \left(m_{22}vr - d_{11}u + \tau_u + \tau_{1dis} - \dot{u}_d m_{11}\right) / m_{11} \tag{35}$$

Let $S_{u1} = 0$, suppose $|\tau_{1dis} - \dot{u}_d m_{11}| < +\infty$, combined with Eq. (35), obtain the equivalent control law:

$$\begin{aligned} \tau_u =& - m_{22}vr + d_{11}u - m_{11}\frac{\alpha_0}{k_{u1}}\left(e^{k_{u1}|u_E|} - 1\right) sgn\left(u_E\right) \\ &- m_{11}\frac{\beta_0}{k_{u1}}\left(1 - e^{-k_{u1}|u_E|}\right)^{q_0/p_0} e^{k_{u1}|u_E|} sgn\left(u_E\right) \end{aligned} \tag{36}$$

For proof τ_u makes u_E the final stabled, design the Lyapunov function:

$$V_{u1} = \frac{1}{2} m_{11} u_E^2 \tag{37}$$

Taking the time derivative of V_{u1}, combined with the Eqs. (35) and (36), we get

$$\begin{aligned} \dot{V}_{u1} =& - \frac{\alpha_0}{k_{u1}}\left(e^{k_{u1}|u_E|} - 1\right)|u_E| \\ &- \frac{\beta_0}{k_{u1}}\left(1 - e^{-k_{u1}|u_E|}\right)^{q_0/p_0} e^{k_{u1}|u_E|}\,|u_E| \\ &+ \left(\tau_{1dis} - \dot{u}_d m_{11}\right) u_E \end{aligned} \tag{38}$$

Because $\dot{u}_d = -k_1\dot{h}_{xe} + u_r r\cos\left(\dot{\psi} - \dot{\psi}_r\right)$, suppose that $\dot{h}_{xe} < +\infty, \dot{\psi}_r < +\infty$, so $|\ \tau_{1dis} - \dot{u}_d m_{11}\ | < +\infty$, and

$$\begin{cases} e^{k_{u1}|u_E|} - 1 \geq 0 \\ 1 - e^{-k_{u1}|u_E|} \geq 0 \end{cases} \tag{39}$$

Therefore, only need to adjust the appropriate α_0 and β_0 to make $\dot{V}_{u1} < 0$, that is making u_E asymptotically stable.

(B) Steering control law τ_r design

Taking the second derivative of $\psi_E = \psi - \psi_d$ in time, we get

$$\begin{cases} \dot{\psi}_E = r - \dot{\psi}_d \\ \ddot{\psi}_E = \dot{r} - \ddot{\psi}_d \end{cases} \tag{40}$$

Where r is not directly controllable, only $\dot{r}$ is directly controllable, so the second-order exponential dynamic sliding mode surface is selected as:

$$\begin{cases} S_{r0} = \dot{\psi}_E + \dfrac{\alpha_1}{k_{r1}}\left(e^{k_{r1}|\psi_E|} - 1\right) sgn\left(\psi_E\right) \\ \qquad + \dfrac{\beta_1}{k_{r1}}\left(1 - e^{-k_{r1}|\psi_E|}\right)^{q_1/p_1} e^{k_{r1}|\psi_E|} sgn\left(\psi_E\right) \\ S_{r1} = k_3 \dot{S}_{r0} + \dfrac{\alpha_1}{k_{r1}}\left(e^{k_{r1}|S_{r0}|} - 1\right) sgn\left(S_{r0}\right) \\ \qquad + \dfrac{\beta_1}{k_{r1}}\left(1 - e^{-k_{r1}|S_{r0}|}\right)^{q_1/p_1} e^{k_{r1}|S_{r0}|} sgn\left(S_{r0}\right) \end{cases} \tag{41}$$

Combining $\ddot{\psi}_E = \dot{r} - \ddot{\psi}_d$ with Eq. (5), we can get

$$\ddot{\psi}_E = \left(\left(m_{11} - m_{22}\right) uv - d_{33} r + \tau_r + \tau_{3dis} - \ddot{\psi}_d m_{33}\right) / m_{33} \tag{42}$$

Let $S_{r1} = 0$, according to the previous section, we can also prove $|\tau_{3dis} - \ddot{psi}_d m_{33}| < +\infty$. Through the joint Eqs. (41) and (42), we can get the equivalent control law:

$$\begin{aligned} \tau_r = & \left(m_{22} - m_{11}\right) uv + d_{33} r - m_{33} \frac{\alpha_1}{k_{r1}}\left(e^{k_{r1}|\psi_E|} - 1\right) sgn\left(\psi_E\right) \\ & - m_{33}\alpha_1 e^{k_{r1}|\psi_E|} - m_{33}\frac{\beta_1}{k_{r1}}\left(1 - e^{-k_{r1}|\psi_E|}\right)^{q_1/p_1} \\ & \left(e^{-k_{r1}|\psi_E|} sgn\left(\psi_E\right) + m_{33} k_{r1} e^{k_{r1}|\psi_E|}\right) \\ & - m_{33}\frac{q_1\beta_1}{p_1} e^{k_{r1}|\psi_E|} sgn\left(\psi_E\right)\left(1 - e^{-k_{r1}|\psi_E|}\right)^{(q_1 - p_1)/p_1} \\ & \left(sgn\left(\psi_E\right) e^{-k_{r1}|\psi_E|}\right) - m_{33}\frac{\alpha_1}{k_{r1}}\left(e^{k_{r1}|S_{r0}|} - 1\right) sgn\left(S_{r0}\right) \\ & - m_{33}\frac{\beta_1}{k_{r1}}\left(1 - e^{-k_{r1}|S_{r0}|}\right)^{q_1/p_1} e^{k_{r1}|S_{r0}|} sgn\left(S_{r0}\right) \end{aligned} \tag{43}$$

Proving that τ_r makes ψ_E finally stable, and designing the Lyapunov function:

$$V_{r1} = \frac{1}{2} m_{33} S_{r0}^2 + \frac{1}{2}\psi_E^2 \tag{44}$$

Taking the time derivative of V_{r1} and combine the Eqs. (41), (42) and (43) to get

$$\begin{aligned} \dot{V}_{r1} = & -\frac{\alpha_1}{k_{r1}}\left(e^{k_{r1}|S_{r0}|} - 1\right)|S_{r0}| - \frac{\beta_1}{k_{r1}}\left(1 - e^{-k_{r1}|S_{r0}|}\right)^{q_1/p_1} \\ & e^{k_{r1}|S_{r0}|}|S_{r0}| - \frac{\alpha_1}{k_{r1}}\left(e^{k_{r1}|\psi_E|} - 1\right)|\psi_E| \\ & - \frac{\beta_1}{k_{r1}}\left(1 - e^{-k_{r1}|\psi_E|}\right)^{q_1/p_1} e^{k_{r1}|\psi_E|}|\psi_E| \\ & + \left(\tau_{3dis} - \ddot{\psi}_d m_{33} + \psi_E\right) S_{r0} \end{aligned} \tag{45}$$

Because $|\psi_E| < +\infty$, combined with Eq. (39), and adjust the appropriate α_1, β_1 and k_{r1} to make S_{r0} and r finally stabilized according to the derivation process in the previous section, then $\dot{V}_{r1} < 0$, that is the system will eventually be uniformly and gradually stabilized.

5 Numerical Simulation

This chapter verifies the effectiveness and robustness of the under-actuated trajectory tracking controller proposed in this paper through a series of designed numerical simulation experiments. CyberShip II is selected as the under-driven USV for testing as showed in the Fig. 2.

Fig. 2 The USV employed in test

According to [27], the dynamic parameters of the mathematical model of USV are set as follows:

$$m_{11} = 25.8\ kg, m_{22} = 33.8\ kg, m_{33} = 2.76\ kg;$$
$$d_{11} = 0.72\ kg/s, d_{22} = 0.8896\ kg/s, d_{33} = 1.9\ kg/s.$$

Set the disturbance of the unmodeled part as:

$$\begin{cases} f_1 = -0.2d_{11}u^2 - 0.1d_{11}u^3 \\ f_2 = -0.2d_{22}v^2 - 0.1d_{22}v^3 \\ f_3 = -0.2d_{33}r^2 - 0.1d_{33}u^3 \end{cases} \tag{46}$$

The disturbance of the external environment is

$$\begin{cases} d_1 = 1 + 1.5\sin(0.2t) + 0.5\cos(0.5t) \\ d_2 = 1 + 1.2\sin(0.1t) + 0.1\cos(0.4t) \\ d_3 = 1 + 1.3\sin(0.5t) + 0.2\cos(0.3t) \end{cases} \tag{47}$$

The resultant force of the total disturbance can be obtained as:

$$\begin{cases} \tau_{1dis} = f_1 + d_1 \\ \tau_{2dis} = f_2 + d_2 \\ \tau_{3dis} = f_3 + d_3 \end{cases} \tag{48}$$

Simulation is carried out through Simulink in MATLAB platform, and the block diagram of Simulink is designed as shown in Fig. 3. The parameters received by the controller of the underactuated USV include the change rate of the reference trajectory, the errors between the motion state of the reference trajectory and that of the agent. The motion state includs dynamic state and kinematic state. The outputs τ_u and τ_r of the controller are calculated by the control algorithm proposed above. The new motion state of the agent is obtained after τ_u and τ_r are input into the motion mathematical model of the agent. The coordinates of x and y axes in the inertial coordinate system are selected for visualization.

The parameters of the exponential dynamic sliding mode controller designed for τ_u are

$$k_1 = 0.5, k_{u1} = 0.3, \alpha_0 = 3, \beta_0 = 3, q_0 = 5, p_0 = 7.$$

The parameters of the exponential dynamic sliding mode controller designed for τ_r are

$$k_2 = 2, k_3 = 0.5, k_{r1} = 0.3, \alpha_1 = 6, \beta_1 = 6, q_1 = 5, p_1 = 7.$$

The limit value of the output control laws τ_u and τ_r are set as follows:

$$\begin{aligned} \tau_{umax} = 250\ N,\ \tau_{umin} = -250\ N, \\ \tau_{rmax} = 450\ N \cdot m,\ \tau_{rmin} = -450\ N \cdot m. \end{aligned}$$

In the simulation, in order to verify the trajectory tracking effect of the controller, a linear trajectory and a sine trajectory are set for verification. Their mathematical expressions are (49) and (50) respectively:

$$\begin{cases} x_r = t \\ y_r = 0.5t \end{cases} \tag{49}$$

$$\begin{cases} x_r = t \\ y_r = 40\sin(0.01t) \end{cases} \tag{50}$$

In order to prove that the designed exponential dynamic sliding mode controller has a better convergence effect, compare it with the global integral sliding mode controller designed in [25], and set the initial state of the USV:

$$\begin{aligned} x(0) = 0\ m, y(0) = 0\ m, \psi = pi/2\ rad, \\ u(0) = 0\ m/2, v(0) = 0\ m/w, r = 0\ rad/s. \end{aligned}$$

The tracking trajectory of the exponential sliding mode controller used in this paper and the ordinary sliding mode controller on the linear trajectory under the condition of no disturbance are showed in Fig. 4. It can be seen from the figure that the exponential sliding mode controller and global integral sliding mode controllers all have good tracking effect on straight trajectories under the condition of no disturbance. However, it can be seen from the tracking error diagram in Fig. 5 that compared with the global integral sliding mode controller, the exponential sliding mode controller has a better tracking effect.

The tracking trajectory of the linear trajectory by the exponential sliding mode controller and the ordinary sliding mode controller with the disturbance situation setting as mentioned above are showed in Fig. 6. After the disturbances setting, compared with the exponential sliding mode controller and the global integral sliding mode controller under the condition of no disturbance, the agent suffer different degrees of influence on the tracking of the trajectories. No matter the trajectory diagram in Fig. 6 or the tracking error diagram in Fig. 7, all can be clearly seen that the exponential sliding mode controller has better anti-interference ability than the global integral sliding mode.

It can be seen from Fig. 8 and Fig. 9 that both the exponential sliding mode controller and the global integral sliding mode controller have good tracking effects on the sine curve in the absence of disturbances. But the exponential sliding mode controller shows the obvious advantages on tracking ability.

After setting the disturbances, it can be seen from Fig. 10 and Fig. 11 that the global integral sliding mode controller has a large error in the tracking of the sine curve, while the exponential sliding mode controller makes a rapid adjustment after a large error to make

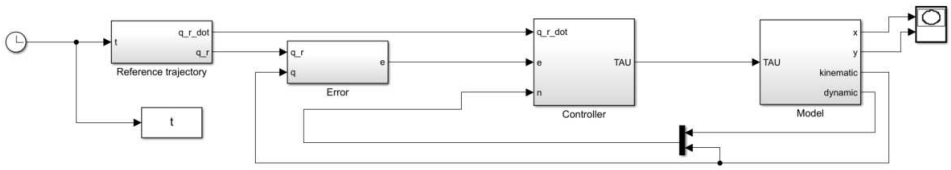

Fig. 3 Simulink block diagram of the numerical test

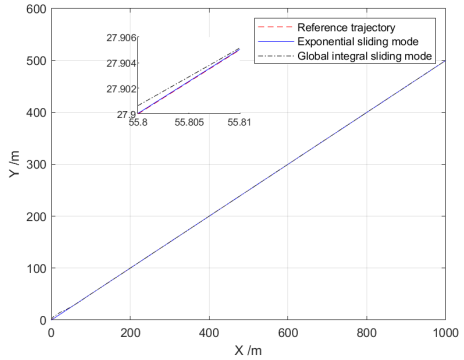

Fig. 4 Tracking performance results of line trajectory without disturbances

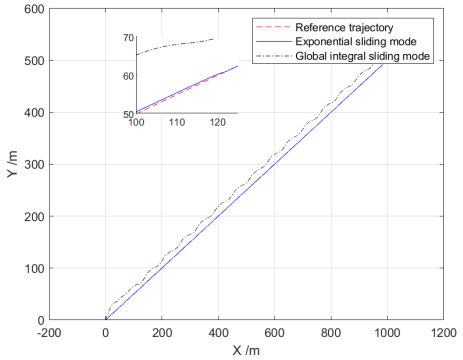

Fig. 6 Tracking performance results of line trajectory without disturbances

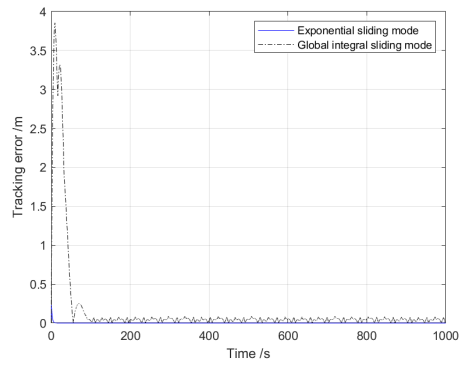

Fig. 5 Tracking error result of line trajectory without disturbances

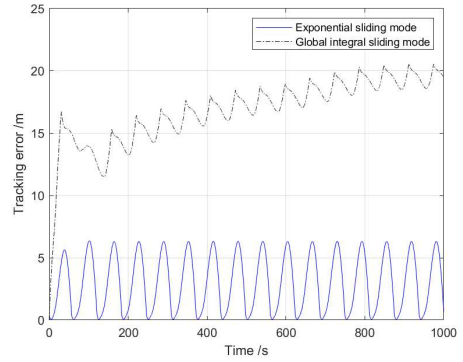

Fig. 7 Tracking error result of line trajectory without disturbances

the error quickly converges to 0. The exponential sliding mode controller shows a better robust effect.

Fig. 12 and Fig. 13 respectively show the output control force and torque changes of the USV under the disturbance condition on the line trajectory and sine trajectory. The results show that the control outputs τ_u and τ_r of the two controllers have reached saturation at the initial stage of control, and then dropped rapidly. In the tracking process, the two control variables are basically kept within 10 units. The initial surge is mainly because a larger gain or difference produces a larger initial value that exceeds the limit of the propulsion system, but does not affect the controller stability. In short words, the trajectory tracking controller designed in this paper has good tracking convergence performance.

6 Conclusion

Though using the tracking controller proposed in this paper, the trajectory tracking control of the USV can berealized. Based on the Lyapunov function, the virtual control variables are determined by the backstepping

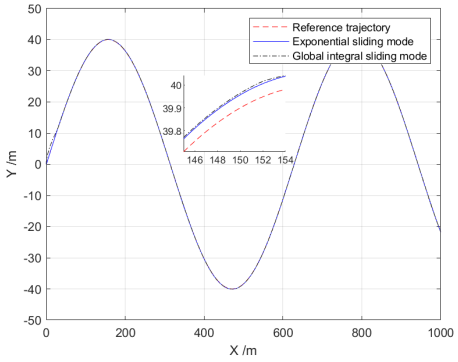

Fig. 8 Tracking performance results of sine trajectory without disturbances

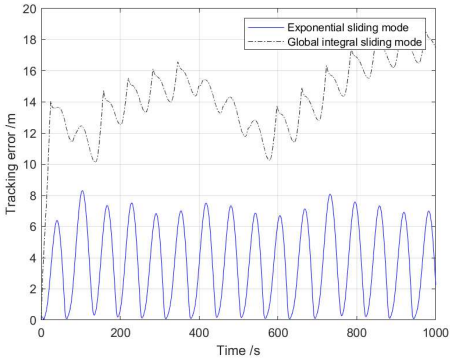

Fig. 11 Tracking error results of sine trajectory with disturbances

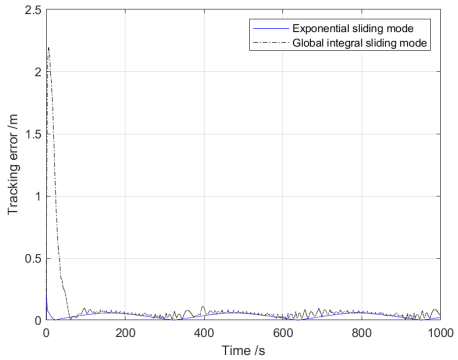

Fig. 9 Tracking error results of sine trajectory without disturbances

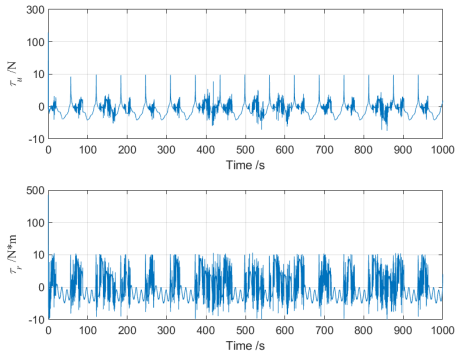

Fig. 12 The output of the line trajectory tracking controller with disturbances

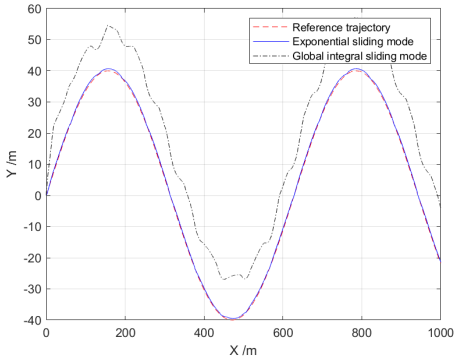

Fig. 10 Tracking performance results of sine trajectory with disturbances

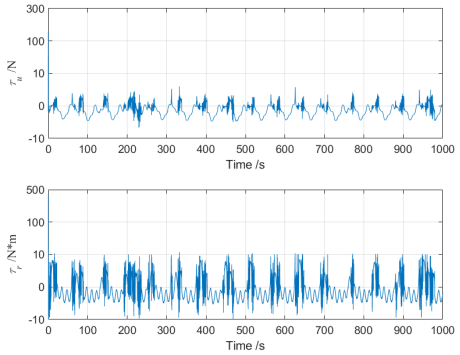

Fig. 13 The output of the sine trajectory tracking controller with disturbances

method to be the propulsion control and the heading deviation respectively, and then the exponential mode sliding controller is analyzed, and the second order is designed by deriving the second order of the exponential mode sliding controller. The exponential sliding mode surface is solved to obtain the control laws, and their stability is analyzed through the Lyapunov function. In order to further prove the effectiveness and robustness of the controller, the tracking simulation experiment of the linear trajectory and the sinusoidal trajectory with two different curvature trajectories is carried out, and the simulation is also performanced under the unmodeled disturbance and the external environment disturbance. By comparing with the global integral sliding mode controllers, the simulation results prove that the trajectory tracking controller of the USV proposed in

this paper is more superior, which supplements the related research.

Acknowledgements This paper is supported by the results of the research project funded by the Shanghai High-level local University Innovation team (Maritime safety and security).

Declarations

Conflict of interest The authors declare that they have no conflict of interest.

Data availability Data sharing not applicable to this article as no datasets were generated or analyzed during the current study

References

1. C. Zhou, S. Gu, Y. Wen, Z. Du, M. Zhu, Ocean Engineering **200**, 107043 (2020)
2. C. Specht, E. Switalski, M. Specht, Polish Maritime Research **24**(3), 36 (2017)
3. A.J. Shafer, M.R. Benjamin, J.J. Leonard, J. Curcio, IEEE (2009)
4. V. Jorge, R. Granada, R. Maidana, D. Jurak, G. Heck, A. Negreiros, S.D. D, L. Gonçalves, A. Amory, Sensors **19**(3) (2019)
5. E. Lefeber, K.Y. Pettersen, H. Nijmeijer, IEEE Trans on Control Systems Technology **11**(1), 52 (2003)
6. C. Paliotta, E. Lefeber, K.Y. Pettersen, in *Decision & Control* (2016)
7. C. Paliotta, E. Lefeber, K.Y. Pettersen, IEEE Trans on Control Systems Technology **27**(4), 1423 (2019)
8. P. Culverhouse, C. Yang, A.S.K. Annamalai, R. Sutton, Journal of Intelligent & Robotic Systems: Theory & Application **78**(2), 319 (2015)
9. L. Liu, Z. Liu, J. Zhang, Abstract and Applied Analysis,2014,(2014-7-14) **2014**, 1 (2014)
10. C. Liu, H. Zheng, R.R. Negenborn, X. Chu, W. Le, in *International Conference on Computational Logistics*, vol. 9335 (2015), vol. 9335, pp. 166–180
11. S.R. Oh, J. Sun, Ocean Engineering **37**(2-3), 289 (2010)
12. V. Djapic, D. Nad, in *Proceedings of the 2010 American Control Conference* (2010), pp. 5997–6003
13. Z. Dong, L. Wan, Y. Li, T. Liu, G. Zhang, International Journal of Naval Architecture and Ocean Engineering **7**(5), 817 (2015)
14. J. Guo, European Journal of Control **57**, 172 (2021)
15. V.K. Tripathi, A.K. Kamath, L. Behera, N.K. Verma, S. Nahavandi, IET Control Theory & Applications **14**(16), 2359 (2020)
16. L.R. Ovalle, R. Héctor, M.A. Llama, Control Engineering Practice **90**, 342 (2019)
17. H.W. Kim, J. Lee, International Journal of Naval Architecture and Ocean Engineering **11**, 2851 (2019)
18. X. Jian, W. Man, Q. Lei, Ocean Engineering **105**, 54 (2015)
19. X. Sun, G. Wang, Y. Fan, Nonlinear Dynamics **106**(3), 2277 (2021)
20. Z. Sun, G. Zhang, L. Qiao, W. Zhang, Journal of Marine Science & Technology **23**(4), 950 (2018)
21. S.T. Venkataraman, S. Gulati, Journal of Dynamic Systems Measurement and Control **115**(3), 5891 (1992)
22. H. GUAN, J. AI, Journal of Guangxi University(Nat Sci Ed) **43**(6), 2172 (2018)
23. Y. Kang, H. Xi, H. Ji, J. Wang, Journal of University of Science and Technology of China **33**(6), 718 (2003)
24. J. Liang, H. Tan, Z. Fan, Journal of University of Electronic Science and Technology of China **40**(1), 11 (2011)
25. X. Sun, G. Wang, Y. Fan, D. Mu, B. Qiu, Applied Sciences **8**(6), 926 (2018)
26. Y. Jiang, C. Guo, H. Yu, in *The 30th Chinese Control and Decision Conference (2018 CCDC)* (2018), pp. 5786–5791
27. B. Qiu, G. Wang, Y. Fan, D. Mu, X. Sun, Applied Sciences **9**(6), 1240 (2019)